Globally Consistent Assessment of Coastal Eutrophication

Elígio Maúre (eligiomaure@gmail.com)
Northwest Pacific Region Environmental Cooperation Center https://orcid.org/0000-0003-0505-3796
Genki Terauchi
Northwest Pacific Region Environmental Cooperation Center
Joji Ishizaka
Institute for Space-Earth Environmental Research, Nagoya University https://orcid.org/0000-0003-0398-1572
Nicholas Clinton
Google, Inc
Michael DeWitt
Google

Article

Keywords: Eutrophication, Potential, Assessment, Water Quality, Global Coastal Oceans, Satellite Chlorophyll, Google Earth Engine, Sustainable Development Goals

Posted Date: June 28th, 2021

DOI: https://doi.org/10.21203/rs.3.rs-421800/v2

Abstract

Eutrophication associated with increasing anthropogenic nutrient loading is an emerging global concern. Often, eutrophication is concomitant with negative impacts on ecosystems and human well-being. Nevertheless, the impacts and the extent of eutrophication are limited to regions with dedicated monitoring programmes. Here we introduce the Global Eutrophication Watch, the first global and interactive assessment map of coastal eutrophication potential (CEP). It is constructed on Google Earth Engine and it evaluates temporal trends in satellite chlorophyll-a (CHL), a proxy for phytoplankton biomass, to devise a global map of CEP. Our analyses suggest that, globally, coastal waters (depth ≤200 m) covering ~1.15 million km2 are eutrophic potential. We found that waters associated with CHL increasing trends—those with potential for further deterioration of water quality—are twofold higher than those showing signs of recovery. The tool effectively identified areas of known eutrophication with severe symptoms, such as dead zones, as well as those with limited to no information of the eutrophication. Our tool introduces the prospect for a consistent global assessment of eutrophication trends with major implications for monitoring Sustainable Development Goals (SDGs). This work contributes to the application of Earth Observations in support of SDGs.

Introduction

Coastal ecosystems provide innumerable services that make them major environmental and economic assets globally[1]. However, their integrity is increasingly threatened by impacts of human activities[2]. Anthropogenic nutrient enrichment, for instance, can stimulate phytoplankton growth. While this growth of phytoplankton can initially be beneficial to the ecosystem, continuous accumulation of organic matter can lead to eutrophication of the system with a series of undesirable ecological effects that can also be harmful to humans. Defined as *the increase in the rate of organic matter supply to water bodies*[3] the definition of eutrophication has been expanded to meet both scientific and legal requirements[4]. This cultural eutrophication associated with excessive or disproportionate nutrient loading is known for its modifications of nutrient levels and structures including a selective magnification of nitrogen and phosphorus supply but reduction of silica[5]. These conditions can trigger a chain of biogeochemical feedback including shifts in phytoplankton composition, formation and persistence of harmful algal blooms (HABs) and hypoxic waters[6–9]. The increased incidence of oxygen deficit waters (hypoxic waters), in turn, can stimulate the proliferation of hypoxia-tolerant species such as *Noctiluca scintillans*[10,11]. Furthermore, eutrophication can also increase the possibility of jellyfish outbreaks[12], can contribute to ocean acidification[7] and to degradation of shallow water habitats[13,14], such as submerged vegetation. Submerged vegetation can also display an array of direct and indirect responses to nutrient loadings that ultimately may lead to their loss, as seen in some seagrass meadows[13]. Thus, continued monitoring of coastal waters with ongoing or highly potential eutrophication is essential to guide activities aimed at preventing or reducing the impacts of the widespread eutrophication of coastal ecosystems.

The UNEP's (United Nations Environmental Programme) workgroup on Sustainable Development Goal (SDG) 14 has been discussing methodologies applicable to the global assessment of coastal eutrophication. Chlorophyll-*a* is listed as one of the parameters for the index of coastal eutrophication potential[15]. In fact, the Global Climate Observing System recognises chlorophyll-*a* concentration—a proxy for phytoplankton biomass—as an Essential Climate Variable[16,17]. It is an important parameter for the characterization of the climate system and its changes, as well as for the study of different factors affecting the dynamics of marine ecosystems including those of anthropogenic origin. The use of chlorophyll-*a* concentration in eutrophication assessment partly relies on the fact that it increases with phytoplankton proliferation and correlates with nutrient loading[18,19]. Furthermore, chlorophyll-*a* shows a long-term response to eutrophication[20,21]. Hence, chlorophyll-*a* is a potential parameter for a preliminary assessment of coastal eutrophication. On the global scale, satellite chlorophyll-*a* (CHL) data from ocean colour observations provide greater spatial and temporal advantages over the conventional ship-based sampling.

The NOWPAP (Northwest Pacific Action Plan, part of the UNEP Regional Seas Programme) developed a Common Procedure for eutrophication assessment (see *Materials and Methods* for details) that includes CHL in its screening process. This Common Procedure is applied in preliminary eutrophication assessment studies in the NOWPAP region[22,23] and was effective in discriminating both eutrophication potential (see *Materials and Methods* for definitions of eutrophic and eutrophication) waters as well as those in recovery[23]. In many coastal regions throughout the globe, however, the information on the status and degree of eutrophication is limited. This study applied the above methodology—the NOWPAP Eutrophication Assessment Tool (NEAT)—and constructed a tool on the Google Earth Engine (GEE)[24] cloud environment for the global screening of coastal eutrophication potential (CEP) using CHL data. Our eutrophication assessment tool (the Global Eutrophication Watch) allows a globally consistent assessment of eutrophication trends in a way never done before. The findings have major implications for monitoring SDGs and can be put into practice by comparing the results from our approach with those obtained from *in-situ* measurements, model simulations, etc., and can also put *in-situ* results into a wider context. On the other hand, there are many regions lacking routine water quality measurements where our tool provides the first global map of CEP and will guide in developing monitoring programmes regionally. Our study contributes towards the use of Earth Observations in support of the SDGs, specifically SDG 14: Life Below Water (with the target to conserve and sustainably use the oceans, seas and marine resources), indicator 14.1.1a "Index of coastal eutrophication".

Results And Discussion

The paper introduces a consistent global assessment method for CEP. The usefulness of the tool is demonstrated by a case study in the Bohai Sea (Figure 1). The Bohai Sea is a semi-enclosed marginal sea, one of the China seas, that has been severely impacted by human activities in the last half century. It has become eutrophic and suffers from symptoms of eutrophication that are well-documented[8,9,25]. Therefore, it provides a good opportunity to compare the eutrophication potential map from our tool with

data from the available literature. Details about the dataset used in this case study and the definitions adopted for the terms eutrophic and eutrophication, as discussed in the following sections, are given in the *Materials and Methods section.*

2.1 Assessment of Coastal Eutrophication Potential: A Case Study in the Bohai Sea

The maps from the global eutrophication watch (Figure 1) covering two assessment periods, 1998-2015 and 1998-2019, revealed that some coastal waters associated with high CHL (>5 mg m^{-3}) and increasing temporal trends (HI) have significantly shrunk while some low CHL with no trends (LN) and low CHL with decreasing trends (LD) have expanded in the Bohai Sea. Overall, the area covered by pixels associated with eutrophication potential (LI, HI) shrank ~27%, whereas for those associated with oligotrophication potential (LD, HD) had a threefold increase between the two assessment periods (Figure 1). This, in part, may be indicative of improving water quality. Reports suggest that there have been a series of control measures implemented in China to reduce nutrient emissions from terrestrial sources. These measures apparently are contributing towards reduction of coastal eutrophication in the China seas[21]. In fact, since 2003, both the frequency and the area affected by red tides decreased[9,21]. On the other hand, the changes in these patches can also be an indication of the sensitivity of trend detection to the data length. This study highlights the usefulness of our tool, which identifies the spatial patterns of eutrophication potential using CHL levels and trends over a larger spatial and temporal scales.

The patterns identified in Figure 1 are further corroborated by reports of water quality of the Bohai Sea. As already stated, most of the bays in this sea have been severely impacted by human activities. Particularly, high inputs of dissolved inorganic nitrogen have been observed in recent decades[5,8,9]. Interestingly, the increase in nitrogen inputs continued even when the total river discharge consistently decreased in relation to the 1960s[9]. As a result, several ecological disasters such as the incidence of red-tides and the occurrence of hypoxia and/or anoxia intensified[9,26]. In the case of the assessment map in Figure 1, a patch of HI was effectively identified in the coastal waters off Qinhuangdao. This region has been found to be an oxygen minimum zone in the Bohai Sea. Further, the waters adjacent to this patch constitute a hypoxia hotspot[8]. The above illustrates the suitability of our tool in identifying the spatial distribution of CEP with the application of CHL from satellite ocean colour remote sensing.

The number of pixels associated with increasing CHL trends significantly decreased between the two assessment periods (Figure 1) indicating that there might be some large-scale phenomena driving this shrinkage of increasing trends in the whole Bohai Sea. Atmospheric deposition, which acts on a much larger scale, can be an important nutrient source to the ocean[27]. In the Bohai Sea, the influence of atmospheric deposition is also significant. Observations and simulation results suggest that the atmospheric contribution to dissolved inorganic nitrogen can range from ~25% to 54% of the total[26,28]. As for the flux of particulate phosphorus entering the sea through windblown dust storms, it can be >500

times greater than on normal days[26]. In recent years, however, declines in the frequencies of dust storms and the volume of China's emissions of major anthropogenic air pollutants have been observed[26,29]. The decline in emissions results from the introduction of China's clean air policies in 2010, driving significant reductions in pollutant emissions in the first seven years of its inception[29]. As shown in a modelling study assessing the effects of atmospheric nitrogen deposition on the marine ecosystem in the Bohai Sea[28], the inclusion of the atmospheric deposition can cause an average increase in phytoplankton biomass of >50%. It naturally follows that our latter assessment (Figure 1B), which includes recent years when both dust storms and anthropogenic emissions have markedly reduced, might reflect the long-term changes in atmospheric nutrient deposition. Other large-scale climate processes such as El Niño (La Niña) and Pacific Decadal Oscillation have also been implicated in the dynamics of the Bohai Sea ecosystem[30]. Fan et al. (ref. 30) analysed the spatial and temporal variations of particulate organic carbon (POC) in the Yellow-Bohai Sea over the period 2002–2016. They suggested that the above climate indices impact the surface POC through their influence on water exchange between the Yellow-Bohai Sea and the East China Sea. This water exchange is controlled by the East Asian winter monsoon and its influence on the Yellow Sea Warm Current. The fact that these factors appear to have an indirect influence[30] suggest that atmospheric deposition might be the primary driver of the observed large scale decrease in CHL levels and trends.

Although we speculate about the possible explanations for the CHL variability observed in the Bohai Sea, we emphasize that our procedure is simply meant for initial assessment of CEP. The mechanisms behind the identified patterns are beyond the scope of the tool and that should be supplemented by follow-up studies. Here, we stress the use of CHL estimates from ocean colour remote sensing as the preliminary parameter for a rapid and a consistent assessment of CEP globally. The significance of this approach is in the use of a single parameter that condenses the spatial and temporal information which allows the identification of areas, potentially, in need of preventive management or eutrophication mitigation efforts.

2.2 Assessment of Coastal Eutrophication Potential: Global Ocean

The global map of CEP (Figure 2A) is composed mostly of LN and HI (Table 1). Pixels associated with high CHL are mostly found in coastal and inland waters. Here, we only focus on the coastal waters (depth ≤ 200 m). To get an intuition of the global distribution of area covered by each eutrophication potential waters, the area estimate was obtained through the combined use of bathymetry data and the marine biogeochemical provinces[31]. Our analysis suggested that globally LI and HI (~799,305 km^2) occupy a larger fraction of coastal waters than LD and HD (~602,406 km^2). The major fraction of both LD-HD and LI-HI combined was found in coastal provinces of Asia (SUND, Table 1). However, the HI class was predominant in the Atlantic Ocean where some of the well-known dead zones, the Gulf of Mexico and the

Baltic Sea, are found[32,33]. Besides the above cases, there are many other coastal seas which were flagged as eutrophication potential (both LI and HI) and are distributed across the globe (Table 1). Although Table 1 also includes coastal upwelling regions, their contribution is relatively smaller than non-upwelling regions. These examples emphasize the utility of the introduced tool in preliminary eutrophication assessment. Not only was the tool able to identify known areas of eutrophication, but also those potentially suffering from the effects of eutrophication in addition to non-reported locations experiencing some level of eutrophication[6,34]. Therefore, the introduction of our Global Eutrophication Watch, a rapid and consistent preliminary assessment of CEP is now globally feasible. This tool should instigate a concerted action against the proliferation of coastal eutrophication.

Table 1. Global distribution of the area coverage estimates of each eutrophication potential class based on the coastal biogeochemical provinces as in Longhurst (2007).

Total Area Estimate [km^2]								
Province Name	**Code**	**Ocean**	**LD**	**LN**	**LI**	**HD**	**HN**	**HI**
Alaska Downwelling Coastal Province	ALSK	Pacific	9,920	183,293	2,827	148	8,787	227
Australia-Indonesia Coastal Province	AUSW	Indian	9,652	806,935	69,319	202	3,490	327
Benguela Current Coastal Province	BENG	Atlantic	437	43,847	7,938	1,355	67,213	4,542
Brazil Current Coastal Province	BRAZ	Atlantic	6,424	416,745	43,420	659	57,375	10,164
California Upwelling Coastal Province	CCAL	Pacific	15,017	64,733	1,328	903	30,438	1,137
Canary Coastal Province	CNRY	Atlantic	4,481	121,800	5,994	3,323	74,124	2,981
Caribbean Province	CARB	Atlantic	23,965	711,105	41,763	1,464	75,830	15,257
Central American Coastal Province	CAMR	Pacific	51,493	168,289	6,862	496	5,196	103
Chile-Peru Current Coastal Province	CHIL	Pacific	6,559	108,325	3,615	1,450	46,428	2,435
China Sea Coastal Province	CHIN	Pacific	38,415	863,543	56,532	595	31,508	4,546
East Africa Coastal Province	EAFR	Indian	9,790	257,185	6,347	148	7,435	262
East Australian Coastal Province	AUSE	Pacific	6,048	289,005	18,183		58	

East India Coastal Province	INDE	Indian	15,941	214,052	4,760	738	20,183	248
Guianas Coastal Province	GUIA	Atlantic	12,525	354,734	22,682	2,800	122,381	9,079
Guinea Current Coastal Province	GUIN	Atlantic	4,119	150,981	25,115	1,109	85,136	11,468
Kuroshio Current Province	KURO	Pacific	7,552	326,373	25,766	371	4,696	89
Mediterranean Sea, Black Sea Province	MEDI	Atlantic	10,327	426,123	38,027	481	5,458	448
New Zealand Coastal Province	NEWZ	Pacific	4,312	85,754	2,859			
Northeast Atlantic Shelves Province	NECS	Atlantic	45,583	696,349	36,761	3,568	190,774	19,073
Northwest Arabian Upwelling Province	ARAB	Indian	14,759	128,285	4,123	2,117	30,154	1,188
Northwest Atlantic Shelves Province	NWCS	Atlantic	27,986	834,160	39,927	1,082	55,701	2,847
Red Sea, Persian Gulf Province	REDS	Indian	56,697	353,303	4,188	417	4,681	477
Southwest Atlantic Shelves Province	FKLD	Atlantic	11,093	709,303	94,027	13	698	141
Sunda-Arafura Shelves Province	SUND	Pacific	166,659	3,298,508	125,220	2,758	71,585	7,181
West India Coastal Province	INDW	Indian	13,337	248,278	16,975	3,120	28,645	528

In addition to the global map of eutrophication potential, we also compared the assessment results based on our improved CHL introduced in 2.1 vs. the standard MODISA CHL product for the period 2003-2019. Overall, we found the CEP waters identified with YOC CHL (Figure 2B) were also apparent in the standard MODISA product (Figure 2C-D). However, LD waters appeared more than LI in the map generated using the standard CHL. The retrievals of CHL in highly dynamic and optically complex waters such as in coastal waters are challenging. The existing algorithms for atmospheric correction are robust in the open ocean where the ocean colour covaries with phytoplankton concentration[35]. In the case of BS, we have the YOC and some other statistically based CHL retrieval algorithms[36] that best represent the phytoplankton variability. We believe that different regions may also have a CHL product that more accurately suits the characteristics of the designated area. As the global application of our methodology in preliminary assessment of CEP should not be contingent on global standard CHL product, in our GEE-based tool, the Global Eutrophication Watch, there is an option for users to enter the path to their asset (dataset in the GEE) of monthly CHL. This monthly CHL can then be used in the assessment instead of the default datasets.

While the focus is on the preliminary assessment of eutrophication potential, oligotrophication potential (LD, HD) are equally worthy of mention. Under the warming climate, the tropics and subtropics are likely to experience enhanced stratification and reduced nutrient supply to the euphotic layer. As a result, phytoplankton growth will be limited with long-term decline (Figure 2A) associated with decreasing primary production[37]. In coastal and enclosed seas, measures to reduce nutrient loading can lead to decreased phytoplankton concentration or reduce the eutrophication and associated ecological disasters such as the incidence of hypoxic events, though other issues like oligotrophication can emerge[38]. The Seto Inland Sea of Japan experienced severe eutrophication during the high economic growth period of the 1960s and 1970s[39], but now is reported to be undergoing oligotrophication[38]. Significant reductions in nutrient loading along with loss in biodiversity are reported to be the precursors of oligotrophication. Moreover, in the oligotrophication process, changes in the food web structure are suggested to have caused a decrease in fishery production of the Seto Inland Sea[40].

In this study, we introduced the Global Eutrophication Watch, a tool for a preliminary eutrophication assessment solely based on satellite CHL. Although different eutrophication assessment methods exist, especially comprehensive eutrophication assessment methods[41–43], their global application is complicated by the need for extensive and intensive field observation campaigns. So, the significance of our introduced tool is in its simplicity and scale. It only uses satellite CHL to provide a systematic assessment of CEP at a macroscopic (global) and microscopic (regional) levels as well as with sufficient temporal information to allow coastal water managers make informed decisions on where to focus their eutrophication management efforts. In this method, we stress the importance of CHL levels and trends. This combination provides a simple but robust assessment scheme. For instance, low CHL but increasing trends (LI) may inform managers about required management actions to prevent future ecological disasters. This warning might go missing in case only satellite CHL levels[44] are considered. On the other hand, with the sole use of CHL trends, high CHL but no trend waters (HN) can be overlooked. CHL levels

are often linked to phytoplankton biomass, which is also linked to the health of the ecosystem. So, our methodology is inexpensive and robust for a global assessment of CEP.

Overall, we expect this contribution to aid in the many global efforts acting to counter the impacts of nutrient pollution and eutrophication. It is well known that management planning efforts should also incorporate available knowledge, and adapt to changing environmental conditions, while evaluating the effectiveness of implemented measures. Thus, our Global Eutrophication Watch tool, with its ready-to-use map of up-to-date information of the status of CEP, provides the required scientific knowledge to support monitoring programmes, adaptive management, and decision-making. It is also useful for educational purposes and in raising awareness, as it is simple and uses very few resources. A simple internet connection, either on a smartphone or computer, allows one to evaluate eutrophication trends worldwide.

Materials And Methods

In this study we used the NEAT methodology to develop a GEE-based tool for the global detection of CEP (the Global Eutrophication Watch) using satellite CHL. In its screening procedure, the NEAT—a robust satellite-based preliminary assessment tool of eutrophication potential—unifies, in a single map, the temporal and spatial information of the area under consideration. It combines the level and trend of CHL to generate six patterns of water quality[23]. The CHL level generates two patterns based on the CHL concentration (α [mg m^{-3}]), the first being composed by CHL lower than the threshold α, CHL < α (L), and the other by CHL ≥ α (H). The trends have three patterns, namely: waters with decreasing trend (D), with no trend (N), or with increasing (I) trend. In this way, a composite map of six classes can be generated, viz. LD, LN, LI, and HD, HN, HI. Before moving on to the explanation of the meaning of each class, it is worth defining the terms adopted in this paper for clarity. *Eutrophic potential* will be used to indicate a productive system with high CHL, whereas *eutrophication potential* refers to the process of becoming eutrophic or a progression of an already eutrophic water body. In addition to the above definitions, we also introduce *oligotrophication potential* which is associated with a least productive water body. Hence, pixels flagged HD, HN and HI are eutrophic potential with HD indicative of systems under recovery, whereas in LI and HI are eutrophication potential. In HI, the conditions may worsen as the water body is already eutrophic potential. Moreover, LD is suggestive of reversed eutrophication, that is, further oligotrophication. LN and HN are indicative of L and H CHL but stable conditions over the analysis period. It is important to note that classification of waters as being L or H is subject to the consideration of the threshold α, which will vary depending on the conditions of each region. However, the same is not the case for D, N or I. Trends will most probably be impacted by the length of the analysis period and/or other environmental factors controlling the variability of CHL rather than a given α. As such, both LD, LI and HD, HI provide critical information about the eutrophication of the system under scrutiny. The global eutrophication watch, therefore, not only provides important information of areas potentially in need of preventive management efforts, but also helps in evaluating the impacts of measures taken to reduce the effects of eutrophication.

The NEAT procedure uses a threshold of 5 mg m^{-3}, and this threshold is computed based on the most recent 3-year mean data of the analysis period. Nevertheless, this threshold is not fixed, and users are able to adjust the level and the composite period to area specific values as different regions may have different thresholds according to the region's background.

The estimation of trends at pixel level is based on the Sen's slope method[45]—a non-parametric trend estimation method—which detects the presence of monotonic trends in a yearly data record at the 90% significance level. Nonparametric tests provide higher statistical power in the case of nonnormality, as in the case of CHL, and are robust against outliers and large data gaps. Trends estimated below a critical threshold are treated as N (no trend). Moreover, as the focus is on the detection of eutrophication potential with consideration of it being a process occurring over a long-time scale (on the order of years), the temporal trends in CHL are estimated from annual maximum obtained from monthly composites of each considered year. The choice is partly motivated by the fact that the evaluation of existence of monotonic trends can also be statistically challenged by short-term variability in CHL. So, by using annual CHL maximum from monthly composites, we effectively remove the seasonal and short-term variabilities. Doing so, we focus on the CHL peak season. Consequently, the obtained trends reflect the interannual behaviour of the phytoplankton bloom season, assuming that the bloom is manifested as high biomass.

For a global detection of CEP, the Global Eutrophication Watch uses the currently available 17-year record of CHL data from Moderate Resolution Imaging Spectroradiometer on Aqua (MODISA), reprocessing 2018, with a spatial resolution of 4 km (https://oceancolor.gsfc.nasa.gov/reprocessing/r2018/aqua/). The data set is stored in the App's asset and its temporal extension is updated on a yearly basis. In addition, the data sets in the App will also be updated following NASA reprocessings that periodically occur when advances in algorithms or sensor calibration knowledge are shown to significantly improve product quality.

Besides the global detection of eutrophication, a case study was developed in the Bohai Sea (BS), a semi-enclosed marginal sea, one of the China seas, to demonstrate the usefulness to the introduced tool. In coastal regions like BS the retrievals of CHL based on the standard algorithm often fail. So, for this case study, we used the open access, improved CHL data from the Marine Environmental Watch of the NOWPAP (https://ocean.nowpap3.go.jp/). The improved CHL is obtained using a regionally tuned CHL algorithm developed by a project of Yellow Sea Large Marine Ecosystem on Ocean Colour (the YOC algorithm) designed to alleviate the impacts of suspended sediments on CHL retrievals[46]. The YOC algorithm was originally developed using the Sea-viewing Wide Field-of-view Sensor (SeaWiFS) sensor bands[46]. Its application to MODISA data is based on the regression between SeaWiFS and MODISA bands and band ratios. Please see ref. 22 for further. The YOC CHL has been demonstrated superior relative to the standard products[47–49] and thus it is of great value for eutrophication assessment in the NOWPAP region. Users have access to the YOC data from https://ocean.nowpap3.go.jp/.

Given that the global level 3 data constitute our default asset for the global eutrophication assessment, following the case study in the BS (2.1), in 2.2 we briefly compare the trends estimated using the YOC CHL

with those obtained from the global data readily obtainable from the National Aeronautics and Space Administration (NASA) of the U.S. This comparison is essential given that the NASA global standard products are more accessible than any other lower-level (such as level 2) data to non-expert users, including water quality managers and decision makers. In addition, it is the least expensive way for a rapid eutrophication assessment before a thorough investigation can follow.

The Global Eutrophication Watch (Figure 3) on the GEE is composed of three main fields: (1) the data-set specification panel, (2) the selection of trend detection interval and (3) the specification of the CHL composite interval and the threshold selection panels. The data panel allows the selection of two default data sets, that is, MODISA and YOC CHL. In practice, only YOC CHL can be checked as MODISA is the *de facto* default. Moreover, this panel also includes a box for users to enter the path to an Earth Engine asset of monthly CHL for the tool to read and use for the assessment. The option is especially important given the challenges associated with CHL retrievals in the coastal waters. Unlike in the open ocean, where phytoplankton dominate the optical properties or co-vary with other optically active constituents, in coastal waters phytoplankton may vary independently of the optical constituents, and thus the global CHL product may fail to resolve phytoplankton variations[50]. So, this option can be understood as a plug-in that allows users around the globe to conduct the eutrophication assessment based on their own assets. This feature enables users to incorporate regionally improved CHL data while keeping the assessment procedure consistent. This has the immediate impact of allowing consistent results to be obtained from a spectrum of ecosystems with different characteristics. The next panel is used to specify the trend detection interval, the start and end years. This panel also includes a button to toggle views, that is, to split the map into two windows providing a capability for comparative assessment. The impact of inclusion of more years in the trend detection analysis, for instance, can be verified by simply using two different year intervals. Finally, the last user defined parameters are for the CHL threshold. Controls for start and end dates are available for users to indicate the time interval to be used to compute the mean CHL. This is used in conjunction with the cut-off level (threshold) to split L vs. H CHL waters.

References

1. Costanza, R. *et al.* The value of the world's ecosystem services and natural capital. *Nature* **387**, 253–260 (1997).

2. Le Moal, M. *et al.* Eutrophication: A new wine in an old bottle? *Sci. Total Environ.* **651**, 1–11 (2019).

3. Nixon, S. W. Coastal marine eutrophication: A definition, social causes, and future concerns. *Ophelia* **41**, 199–219 (1995).

4. Lemley, D. A. & Adams, J. B. Eutrophication. in *Encyclopedia of Ecology* **1**, 86–90 (Elsevier, 2019).

5. Howarth, R. *et al.* Coupled biogeochemical cycles: Eutrophication and hypoxia in temperate estuaries and coastal marine ecosystems. *Front. Ecol. Environ.* **9**, 18–26 (2011).

6. Diaz, R. J. & Rosenberg, R. Spreading Dead Zones and Consequences for Marine Ecosystems. *Science (80-.).* **321**, 926–929 (2008).

7. Doney, S. C. The growing human footprint on coastal and open-Ocean biogeochemistry. *Science* **328**, 1512–1516 (2010).

8. Wei, Q. *et al.* Spatiotemporal variations in the summer hypoxia in the Bohai Sea (China) and controlling mechanisms. *Mar. Pollut. Bull.* **138**, 125–134 (2019).

9. Xin, M. *et al.* Long-term changes in nutrient regimes and their ecological effects in the Bohai Sea, China. *Mar. Pollut. Bull.* **146**, 562–573 (2019).

10. Gomes, H. do R. *et al.* Massive outbreaks of Noctiluca scintillans blooms in the Arabian Sea due to spread of hypoxia. *Nat. Commun.* **5**, 4862 (2014).

11. Goes, J., Al-hashmi, K. & Buranapratheprat, A. Global Ecology and Oceanography of Harmful Algal Blooms. **232**, (2018).

12. Purcell, J. E. Jellyfish and Ctenophore Blooms Coincide with Human Proliferations and Environmental Perturbations. *Ann. Rev. Mar. Sci.* **4**, 209–235 (2012).

13. Burkholder, J. A. M., Tomasko, D. A. & Touchette, B. W. Seagrasses and eutrophication. *J. Exp. Mar. Bio. Ecol.* **350**, 46–72 (2007).

14. Glibert, P. M. Eutrophication, harmful algae and biodiversity — Challenging paradigms in a world of complex nutrient changes. *Mar. Pollut. Bull.* **124**, 591–606 (2017).

15. UNSD. Workplan on Tier III indicators. **3**, 244 (2017).

16. Bojinski, S. *et al.* The concept of essential climate variables in support of climate research, applications, and policy. *Bull. Am. Meteorol. Soc.* **95**, 1431–1443 (2014).

17. GCOS. Systematic observation requirements for satellite-based data products for climate. 139 (2011).

18. Smith, V. H. Responses of estuarine and coastal marine phytoplankton to nitrogen and phosphorus enrichment. *Limnol. Oceanogr.* **51**, 377–384 (2006).

19. Woodland, R. J. *et al.* Nitrogen loads explain primary productivity in estuaries at the ecosystem scale. *Limnol. Oceanogr.* **60**, 1751–1762 (2015).

20. Anderson, D. M., Glibert, P. M. & Burkholder, J. M. Harmful Algal Blooms and Eutrophication: Nutrient Sources, Composition, and Consequences. *Estuaries* **25**, 704–726 (2002).

21. Wang, B., Xin, M., Wei, Q. & Xie, L. A historical overview of coastal eutrophication in the China Seas. *Mar. Pollut. Bull.* **136**, 394–400 (2018).

22. Terauchi, G., Tsujimoto, R., Ishizaka, J. & Nakata, H. Preliminary assessment of eutrophication by remotely sensed chlorophyll-a in Toyama Bay, the Sea of Japan. *J. Oceanogr.* **70**, 175–184 (2014).

23. Terauchi, G. *et al.* Assessment of eutrophication using remotely sensed chlorophyll-a in the Northwest Pacific region. in *Remote Sensing of the Open and Coastal Ocean and Inland Waters* (eds. Frouin, R. J. & Murakami, H.) 17 (SPIE, 2018). doi:10.1117/12.2324641

24. Gorelick, N. *et al.* Google Earth Engine: Planetary-scale geospatial analysis for everyone. *Remote Sens. Environ.* **202**, 18–27 (2017).

25. Qiao, Y., Feng, J., Cui, S. & Zhu, L. Long-term changes in nutrients, chlorophyll a and their relationships in a semi-enclosed eutrophic ecosystem, Bohai Bay, China. *Mar. Pollut. Bull.* **117**, 222–228 (2017).

26. Wang, J., Yu, Z., Wei, Q. & Yao, Q. Long-Term Nutrient Variations in the Bohai Sea Over the Past 40 Years. *J. Geophys. Res. Ocean.* **124**, 703–722 (2019).

27. Duce, R. A. *et al.* Impacts of atmospheric anthropogenic nitrogen on the open ocean. *Science (80-.).* **320**, 893–897 (2008).

28. Shou, W., Zong, H., Ding, P. & Hou, L. A modelling approach to assess the effects of atmospheric nitrogen deposition on the marine ecosystem in the Bohai Sea, China. *Estuar. Coast. Shelf Sci.* **208**, 36–48 (2018).

29. Zheng, B. *et al.* Trends in China's anthropogenic emissions since 2010 as the consequence of clean air actions. *Atmos. Chem. Phys.* **18**, 14095–14111 (2018).

30. Fan, H., Wang, X., Zhang, H. & Yu, Z. Spatial and temporal variations of particulate organic carbon in the Yellow-Bohai Sea over 2002–2016. *Sci. Rep.* **8**, 7971 (2018).

31. Longhurst, A. R. *Ecological Geography of the Sea*. (Elsevier, 2007). doi:10.1016/B978-0-12-455521-1.X5000-1

32. Rabalais, N. N., Turner, R. E. & Wiseman, W. J. Gulf of Mexico Hypoxia, A.K.A. "The Dead Zone". *Annu. Rev. Ecol. Syst.* **33**, 235–263 (2002).

33. Carstensen, J., Andersen, J. H., Gustafsson, B. G. & Conley, D. J. Deoxygenation of the Baltic Sea during the last century. *Proc. Natl. Acad. Sci.* **111**, 5628–5633 (2014).

34. Levin, L. A. *et al.* Effects of natural and human-induced hypoxia on coastal benthos. *Biogeosciences* **6**, 2063–2098 (2009).

35. Siegel, D. A., Wang, M., Maritorena, S. & Robinson, W. Atmospheric correction of satellite ocean color imagery: the black pixel assumption. *Appl. Opt.* **39**, 3582 (2000).

36. Wang, Y., Liu, D. & Tang, D. L. Application of a generalized additive model (GAM) for estimating chlorophyll-a concentration from MODIS data in the Bohai and Yellow Seas, China. *Int. J. Remote Sens.* **38**, 639–661 (2017).

37. Behrenfeld, M. J. *et al.* Climate-driven trends in contemporary ocean productivity. *Nature* **444**, 752–755 (2006).

38. Yanagi, T. Oligotrophication in the Seto Inland Sea. in 39–67 (Springer, Dordrecht, 2015). doi:10.1007/978-94-017-9915-7_3

39. Imai, I., Yamaguchi, M. & Hori, Y. Eutrophication and occurrences of harmful algal blooms in the Seto Inland Sea, Japan. *Plankt. Benthos Res.* **1**, 71–84 (2006).

40. Yamamoto, T. The Seto Inland Sea - Eutrophic or oligotrophic? in *Marine Pollution Bulletin* **47**, 37–42 (Elsevier Ltd, 2003).

41. Bricker, S. B., Clement, C. G., Pirhalla, D. E., Orlando, S. P. & Farrow, D. R. G. National Estuarine Eutrophication Assessment: Effects of Nutrient Enrichment in the Nation's Estuaries. *NOAA Natl. Ocean Serv. Spec. Proj. Off. Natl. Centers Coast. Ocean Sci.* **Silver Spr**, 71 (1999).

42. Andersen, J. H. *et al.* Development of tools for assessment of eutrophication in the Baltic Sea. *Balt. Sea Environ. Proc.* **104**, 1–64 (2006).

43. NOWPAP CEARAC. *Procedures for assessment of eutrophication status including evaluation of land-based sources of nutrients for the NOWPAP*. (2009).

44. Gohin, F. *et al.* Towards a better assessment of the ecological status of coastal waters using satellite-derived chlorophyll-a concentrations. *Remote Sens. Environ.* **112**, 3329–3340 (2008).

45. Sen, P. K. Estimates of the Regression Coefficient Based on Kendall's Tau. *J. Am. Stat. Assoc.* **63**, 1379–1389 (1968).

46. Siswanto, E. *et al.* Empirical ocean-color algorithms to retrieve chlorophyll-a, total suspended matter, and colored dissolved organic matter absorption coefficient in the Yellow and East China Seas. *J. Oceanogr.* **67**, 627–650 (2011).

47. Yoon, J.-E. *et al.* Assessment of Satellite-Based Chlorophyll-a Algorithms in Eutrophic Korean Coastal Waters: Jinhae Bay Case Study. *Front. Mar. Sci.* **6**, 359 (2019).

48. Xu, Y., Ishizaka, J., Yamaguchi, H., Siswanto, E. & Wang, S. Relationships of interannual variability in SST and phytoplankton blooms with giantjellyfish (Nemopilema nomurai) outbreaks in the Yellow Sea

and East China Sea. *J. Oceanogr.* **69**, 511–526 (2013).

49. Yamaguchi, H. *et al.* Seasonal and spring interannual variations in satellite-observed chlorophyll-a in the Yellow and East China Seas: New datasets with reduced interference from high concentration of resuspended sediment. *Cont. Shelf Res.* **59**, 1–9 (2013).

50. Mouw, C. B. *et al.* Aquatic color radiometry remote sensing of coastal and inland waters: Challenges and recommendations for future satellite missions. *Remote Sensing of Environment* **160**, 15–30 (2015).

Figures

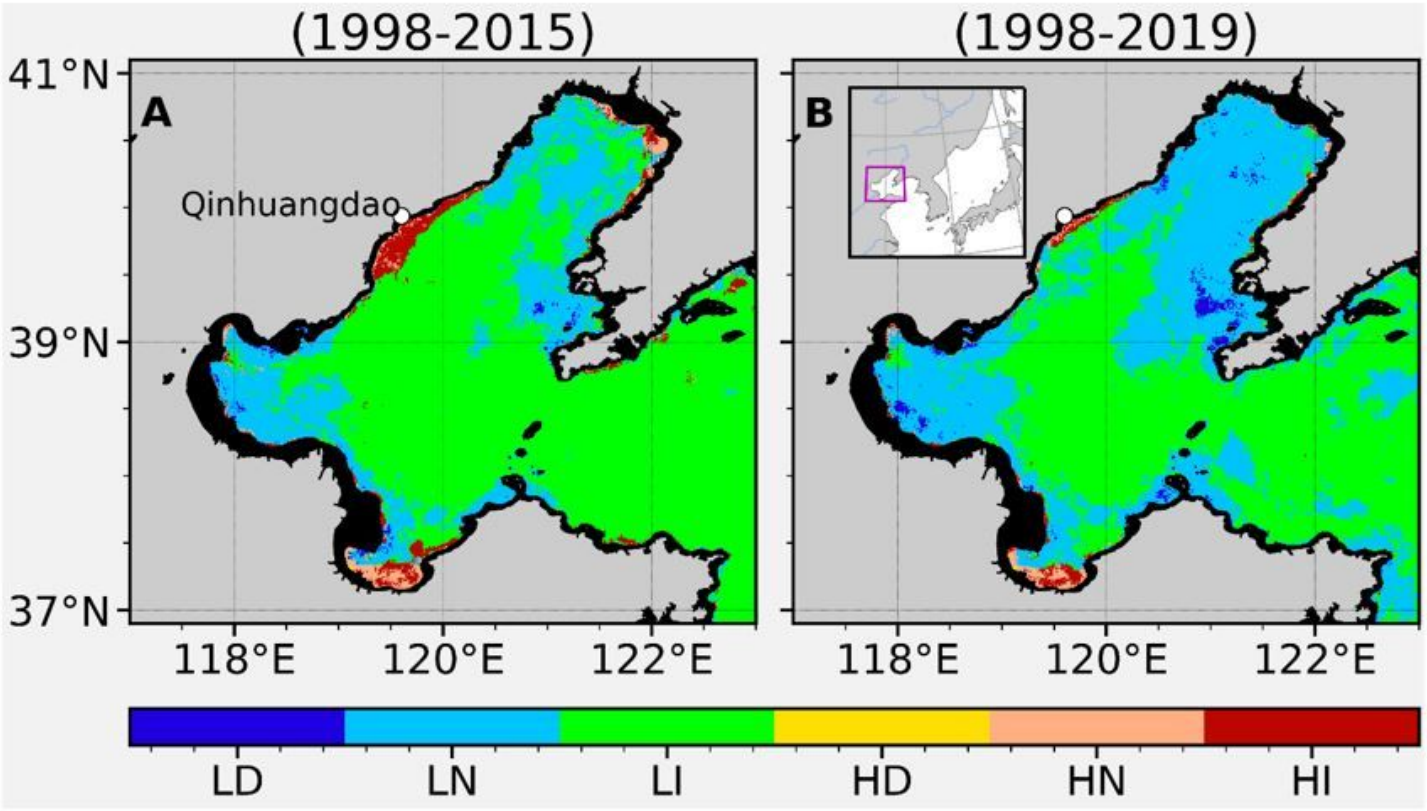

Figure 1

Map of coastal eutrophication potential (CEP) in the Bohai Sea (BS). LD, LN, and LI depict the status as being low CHL (α < 5 mg m−3) with decreasing trend, no trend and increasing trend, respectively. HD, HN and HI indicate high CHL (α ≥ 5 mg m−3) with the three above-mentioned trends, respectively. A. Preliminary assessment of CEP for the period 1998-2015. B. Same as (A) but for the period 1998-2019. The rectangle in magenta (B) shows the location of BS.

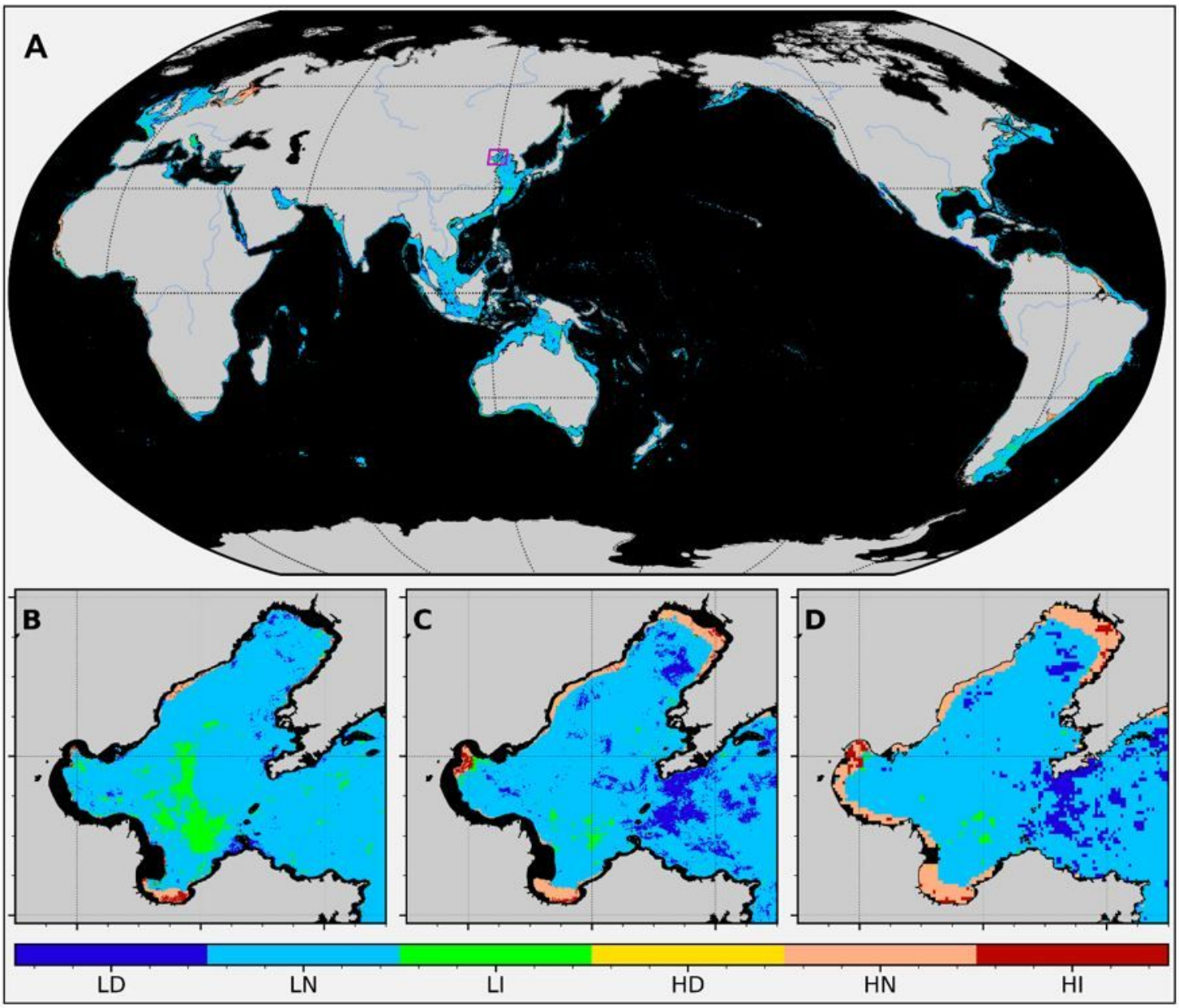

Figure 2

Map of CEP (A) in the global ocean and (B-D) in the BS. A. Preliminary assessment of CEP for the period 2003-2019 based on MODISA global dataset. The CHL threshold is same as in Figure 1. B. Preliminary assessment based on the YOC algorithm for the same period as in (A) but with spatial resolution of 1 km. C. Same as (B) but for MODISA. D. Same as (B) but for MODISA 4 km spatial resolution. The southern and northern regions with few observations (<70% in the 17-year period) were masked. The GEE App is accessible through the link https://ermaure.users.earthengine.app/view/global-eutrophication-watch.